Persistent patterns in transient chaotic fluid mixing

D. Rothstein*, E. Henry* & J. P. Gollub*†

** Department of Physics, Haverford College, Haverford, Pennsylvania 19041, USA*
† Department of Physics, University of Pennsylvania, Philadelphia, Pennsylvania 19104, USA

Chaotic advection[1–3] of a fluid can cause an initially inhomogeneous impurity (a passive scalar field) to develop complex spatial structure as the elements of the fluid are stretched and folded, even if the velocity field is periodic in time. The effect of chaotic advection on the transient mixing of impurities—the approach to homogeneity—has been explored theoretically and numerically[4–8]. A particularly intriguing prediction is the development of persistent spatial patterns, whose amplitude (contrast) decays slowly with time but without change of form. Here we investigate these phenomena using an electromagnetically driven two-dimensional fluid layer in which one half is initially labelled by a fluorescent dye (the passive scalar). We observe the formation of structurally invariant but slowly decaying mixing patterns, and we show how the various statistical properties that characterize the dye concentration field evolve with time as mixing proceeds through many cycles. These results show quantitatively how advective stretching of the fluid elements and molecular diffusion work together to produce mixing of the impurity. We contrast the behaviour of time-period; c flows and identically forced but weakly turbulent flows at lower viscosity, where mixing is much more efficient.

Density stratification and magnetic forcing are used to create a two-dimensional flow with good accuracy. A layer of glycerol–water–salt solution 3 mm deep carries a horizontal electric current in the presence of an array of strong permanent magnets just below the fluid. An ordered square array with alternating polarity, and a spatially disordered array (with magnets having random locations and polarity), are used to create both regular and disordered cellular flows by means of Lorenz forces.

The fluid of interest is a dilute fluorescent dye, contained in a separate 1 mm upper layer of glycerol–water (37% by weight). It is less dense than the glycerol–water–salt solution described above, and the layers remain separate for the duration of an experiment, typically 10 min. The dye diffuses slowly because the Schmidt number (the ratio of kinematic viscosity to dye diffusivity) is about 2,000. The upper layer, which contains no salt, is driven by friction at its lower boundary. This arrangement provides a nearly two-dimensional flow in the upper layer[9,10]. Residual vertical flows are at least an order of magnitude weaker than the horizontal circulation. Only half the upper layer is initially labelled with the dye.

The use of glycerol (32% by volume) suppresses instabilities leading to turbulence by increasing the viscosity to 3.3×10^{-6} m^2 s^{-1}, and thus keeping the Reynolds number well below 100. As a result, when the current is steady (and of the order of 60 mA), the velocity field $\mathbf{v}(\mathbf{r})$ is time-independent. When the current is oscillatory, $\mathbf{v}(\mathbf{r})$ is found to be time-periodic. The fluid cell is placed in the feedback loop of an operational amplifier circuit so that the current accurately follows the applied voltage waveform. For time-periodic square or sine wave forcing there is no mean flow. When the glycerol is omitted, on the other hand, two-dimensional weakly turbulent flows can be created[11].

The fluid is illuminated near 365 nm, and the fluorescent response, imaged by a cooled 12 bit CCD camera operating at 512×512 pixel resolution, is accurately linear in the local concentration under the experimental conditions[10]. The camera is triggered to sample the dye distribution every period or half period.

An example of the mixing process is shown in Fig. 1 for the case of time-periodic forcing at 100 mHz after 20 periods, using a spatially periodic magnet array. The dye solution, initially confined to the right half of the image, is progressively stretched and folded,

Figure 1 Snapshot of the concentration field for transient magnetically forced chaotic mixing. Fluid labelled with fluorescein was initially confined to the right half of the 20×24 cm cell; the imaged region is 9.4×9.4 cm. The light intensity under ultraviolet illumination is shown after 20 periods of forcing by a time periodic electric current at 100 mHz, in the presence of a spatially periodic magnet array. The repetitive stretching and folding that is characteristic of chaotic advection is evident.

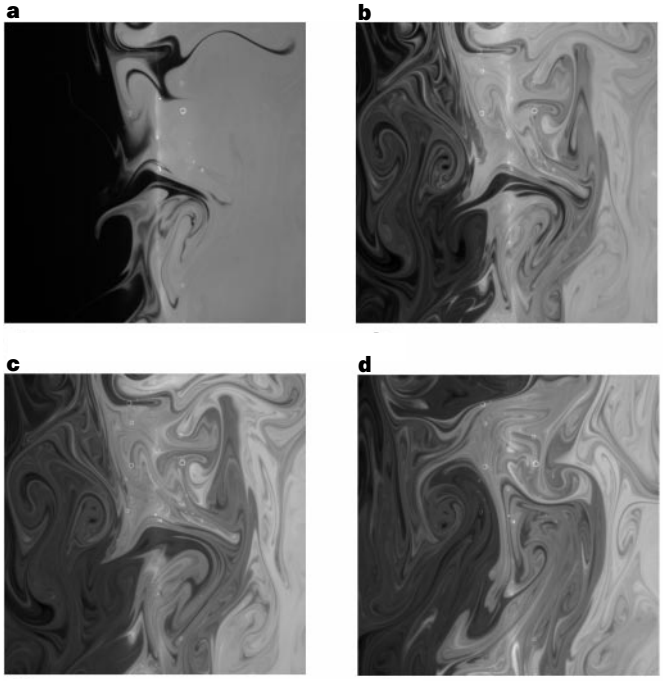

Figure 2 Attainment of a persistent mixing pattern using a disordered array of forcing magnets. The impurity field develops a complex structure after about 10 periods that repeats periodically, except for a gradual loss of contrast. **a–c**, $t = 2$, 20 and 50 periods, respectively. **d**, Sampling out of phase at 50.5 periods shows that the tracer distribution changes substantially within each cycle. The forcing frequency is 70 mHz.

intruding into the left half, while unlabelled fluid penetrates the right half. The underlying forcing vortices are evident from the dye pattern, and the striations are typical of chaotic advection.

The case of time-periodic forcing by a random magnet array is shown as a function of time in Fig. 2, by means of images obtained at constant phase relative to the forcing after 2, 20 and 50 cycles. Remarkably, after about 10 cycles, a complex spatial pattern is reached that subsequently recurs once per period. This may be seen qualitatively by comparing Fig. 2b and c, which are nearly identical, including the fine detail, except for a reduction in contrast over time. The final panel shows the situation one half cycle later at 50.5 cycles, and indicates that the impurity distribution is quite different (though statistically similar) at other phases relative to the forcing.

To demonstrate the approach to a persistent pattern quantitatively, we show (Fig. 3a) the cross-correlation coefficient of images obtained 4 cycles apart, as a function of time from the start of the mixing. This quantity increases rapidly from a low value to about 0.98, showing that images obtained 4 cycles apart are nearly identical after about 10 periods of mixing. A similar result is obtained for images spaced 10 cycles apart. Another way to test for a persistent but slowly decaying pattern is to fit the intensity data to a product of separate space and time functions: $I(r,t) = f(r)g(t) + C$, where the constant C is the intensity after complete mixing. This can be done with a r.m.s. variation of less than 1% for $10 < t < 70$ periods. The resulting function $f(r)$ is similar to Fig. 2c, while the contrast $g(t)$ decays smoothly to zero, leaving a uniform intensity. We find that similar fits can be obtained for the spatially periodic forcing of Fig. 1.

Although the spatial structure approaches an asymptotic form, mixing continues, owing to stretching of fluid elements and diffusion. This may be seen by monitoring the intensity probability distribution function (PDF) and the decay of its normalized variance $\langle(\delta I)^2\rangle$, which is a measure of "unmixedness"[12] or contrast, shown in Fig. 3b. The variance of the PDF shows a pronounced tail, and is approximately described by a power law of the form $bt^{-0.69\pm0.01}$ for $t > 10$, where b is a constant. However, for longer runs, an approximately exponential decay is eventually attained. Also, in Fig. 3b, we show the decay of the variance when the viscosity is reduced so that the flow becomes weakly turbulent at higher Reynolds number, with all forcing parameters the same. The decay is then much faster and is well described as an exponential in time of the form $c\exp[-(0.7 \pm 0.1)t]$. However, there is no well-defined asymptotic pattern for the turbulent case; the concentration field pattern continues to fluctuate strongly. The fluorescent intensity PDFs are also quite different for the two cases: the turbulent flow PDF approaches a gaussian for $t \geqslant 50$, while that for the chaotic flow is complex and broader.

We have tested for the approach to a persistent pattern under a variety of other circumstances: (1) if the forcing frequency is increased, the approach to the asymptotic state requires more cycles because the shorter fluid trajectories before reversal tend to reduce the effective Lyapunov exponent; (2) if the forcing current contains a d.c. component so that there is a mean flow, the results are not substantially changed; (3) we find generally similar (but

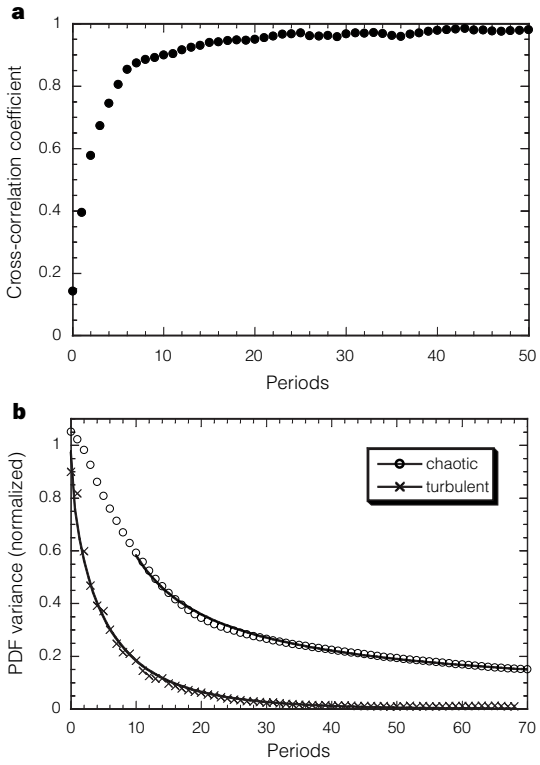

Figure 3 Quantitative characterization of the persistent mixing pattern. **a**, Cross-correlation coefficient between images separated by four periods, as a function of time from the start of mixing, for the chaotic case of Fig. 2. (The intensity is measured with respect to the average along a vertical line, in order to remove spurious correlation due only to the background dye gradient.) The asymptotic value of 0.98 implies that the concentration field returns to almost the same state once per cycle. **b**, Variance $\langle(\delta I)^2\rangle$ of the fluorescent intensity probability distribution function (PDF) versus time, for chaotic mixing as in Fig. 2, and for mixing by weakly turbulent flow at lower viscosity using 70 mHz forcing. The Reynolds number is about ten times larger in the turbulent case. Fits to the data are described in the text.

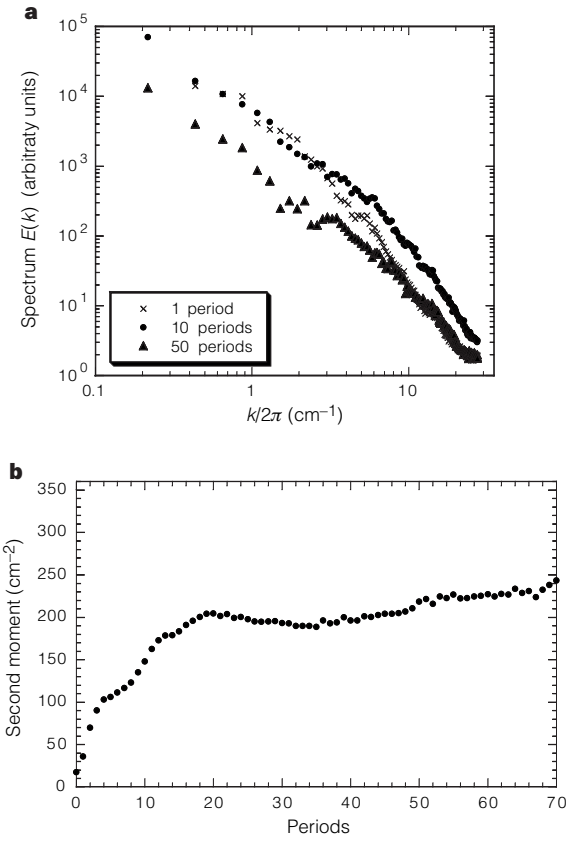

Figure 4 Spatial power spectra and moments for transient mixing. **a**, One-dimensional power spectrum $E(k)$ at several times, for the chaotic advection of Fig. 2. The spectrum widens over the first few periods, as a result of stretching and folding. Later, the shape remains roughly fixed but the overall amplitude decreases with time at all k values. **b**, Second spectral moment as a function of time, showing saturation after about 10 periods.

somewhat slower) mixing for spatially periodic forcing; (4) for temporally non-periodic forcing, there are no recurrences.

The one-dimensional spatial power spectrum $E(k)$ computed in the standard way[10] provides a useful diagnostic for the development of fine structure in the concentration field. An example is shown in Fig. 4a for time-periodic forcing using the spatially disordered magnet array (as in Fig. 2), at several different times. For $l < t < 10$, the high frequency tail of $E(k)$ rises, as stretching and folding produce fine structure. Later, the entire spectrum declines at all frequencies with little further change of shape. The decline at high k is due to diffusion, and the decline at low k is due to the continuing transport of spectral variance to high k by stretching. The spectrum does not follow a well-defined power law (nor is one expected[6] for transient mixing); it is steeper at higher k. The behaviour of the second spectral moment $\langle k^2 \rangle$, shown in Fig. 4b, increases rapidly at first and then essentially saturates, consistent with the asymptotic structure noted earlier.

The fine structure of the dye pattern may also be investigated by studying the PDF of the magnitude of the concentration gradient. An example is shown in Fig. 5 for the same conditions as in Fig. 2. Gradients have been expressed in units of the standard deviation of the concentration field to compensate for the gradual homogenization. It is striking to see that the gradient PDF reaches an invariant form that is essentially identical at $t = 20$ and 50 periods. The distribution at high gradients is accurately exponential. Such exponential tails for distributions of concentration gradients have been noted in several theoretical studies[13]. When the same experiment is done for the weakly turbulent flow at lower viscosity, the resulting distribution is similar to that of Fig. 5 for $t = 10$, but the shape continues to evolve, approaching a maxwellian distribution (characteristic of independent gaussian components) at longer times. Therefore, the large gradients are attenuated more rapidly than are small gradients for the turbulent flow. Diffusion broadens the striations in two-dimensional turbulence, but not in chaotic mixing.

We find that chaotic mixing, produced by time-periodic cellular flows, leads to a remarkable persistent spatial structure, a complex pattern that recurs periodically while its contrast decays slowly with time. The recurrence is surprising (when first encountered) since additional striations are created during each cycle. The corresponding spatial power spectrum retains its shape as it declines simultaneously at all wavenumbers owing to a delicate balance of two distinct processes: stretching and diffusion. The probability distribution of the magnitude of the concentration gradient reaches an invariant form (when suitably normalized) with a peak at non-zero gradient and exponential tails. All of these properties show that the recurrent mixing pattern represents a dynamical non-equilibrium state rather than a static condition. Finally, we note that identically forced but weakly turbulent flows at lower viscosity become homogeneous and transport material much more rapidly than the time-periodic flows manifesting chaotic advection. However, turbulence is generally unavailable when mixing in small scale devices is required. □

Received 3 June; accepted 18 August 1999.

1. Aref, H. Stirring by chaotic advection. *J. Fluid Mech.* **143,** 1–21 (1984).
2. Ottino, J. M. Mixing, chaotic advection, and turbulence. *Annu. Rev. Fluid Mech.* **22,** 207–253 (1990).
3. Fountain, G. O., Khakhar, D. V. & Ottino, J. M. Visualization of three-dimensional chaos. *Science* **281,** 683–686 (1998).
4. Pierrehumbert, R. T. Tracer microstructure in the large-eddy dominated regime. *Chaos Solitons Fractals* **4,** 1091–1110 (1994).
5. Antonsen, T. M., Fan, Z., Ott, E. & Garcia-Lopez, E. The role of chaotic orbits in the determination of power spectra of passive scalars. *Phys. Fluids* **8,** 3094–3104 (1996).
6. Antonsen, T. M. & Ott, E. Multifractal power spectra of passive scalars convected by chaotic fluid flows. *Phys. Rev. A* **44,** 851–857 (1991).
7. Muzzio, F. J., Meneveau, C., Swanson, P. D. & Ottino, J. M. Scaling and multifractal properties of mixing in chaotic flows. *Phys. Fluids A* **4,** 1439–1456 (1992).
8. Alvarez, M. M., Muzzio, F. J., Cerbelli, S., Adrover, A. & Giona, M. Self-similar spatiotemporal structure of intermaterial boundaries in chaotic flows. *Phys. Rev. Lett.* **81,** 3395–3398 (1998).
9. Paret, J., Marteau, D., Paireau, O. & Tabeling, P. Are flows electromagnetically forced in thin stratified layers two-dimensional? *Phys. Fluids* **9,** 3102–3104 (1997).
10. Williams, B. S., Marteau, D. & Gollub, J. P. Mixing of a passive scalar in two-dimensional turbulence. *Phys. Fluids* **9,** 2061–2080 (1997).
11. Paret, J. & Tabeling, P. Experimental observation of the two-dimensional inverse energy cascade. *Phys. Rev. Lett.* **79,** 4162–4165 (1997).
12. Miller, P. L. & Dimotakis, P. E. Reynolds number dependence of scalar fluctuations in a high Schmidt number turbulent jet. *Phys. Fluids A* **3,** 1156–1163 (1991).
13. Shraiman, B. I. & Siggia, E. D. Lagrangian path integrals and fluctuations in random flow. *Phys. Rev. E* **49,** 2912–2927 (1994).

Acknowledgements

We thank J. Andersen, J.-C. Geminard, A. Kudrolli, and W. Losert for experimental contributions, and E. Ott and B. Shraiman for discussions. This work was supported by the Condensed Matter Physics Program of the US NSF.

Correspondence and requests for materials should be addressed to J.P.G. (e-mail: jgollub@haverford.edu).

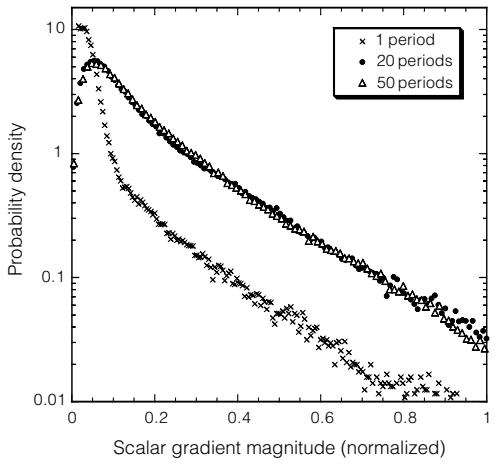

Figure 5 Probability distribution of the magnitude of the concentration gradient for chaotic mixing (Fig. 2). The distribution, here normalized by the standard deviation of the intensity field to compensate for the gradual loss of contrast, reaches an invariant form after about 20 periods, with a peak at finite gradient and an exponential tail.

Sonoluminescence temperatures during multi-bubble cavitation

William B. McNamara III*, Yuri T. Didenko*‡ & Kenneth S. Suslick*

* *Department of Chemistry, University of Illinois at Urbana-Champaign, 600 S. Mathews Avenue, Urbana, Illinois 61801, USA*

Acoustic cavitation—the formation and implosive collapse of bubbles—occurs when a liquid is exposed to intense sound. Cavitation can produce white noise, sonochemical reactions, erosion of hard materials, rupture of living cells and the emission of light, or sonoluminescence[1,2]. The concentration of energy during the collapse is enormous: the energy of an emitted photon can exceed the energy density of the sound field by about twelve orders of magnitude[3], and it has long been predicted that the interior bubble temperature reaches thousands of degrees Kelvin during collapse. But experimental measurements[4,5] of

‡ Permanent address: Pacific Oceanological Institute, Vladivostok 690061, Russia.